

The Evolution of a Two-Dimensional H₂-O₂-Ar Detonation Wave in Pipe Bends

Jian Li, Huilan Ren, Hui Zhao, Jianguo Ning

State Key Laboratory of Explosion Science and Technology, Beijing Institute of Technology
Beijing, China

1 Introduction

Internal detonation is a frequently occurring threat to transport pipelines of natural gas plants. For the purpose of evaluating the response properties of pipe bend wall to detonation wave, many efforts should be made to investigate the research on detonation pressure history and complex wave structures [1]. The study of regular detonation propagating through a pipe bend provides an attractive configuration for research prior, as it combines both diffraction and reflection. Tomas [2] found that, for short radius bend, the behavior on the compressive side is dominated by a re-initiation process at the end of the bend. Deiterding's numerical simulation on the transient detonation structures in H₂-O₂ mixtures in smooth pipe bends [3] showed the formation of transverse detonation waves. Uchida [4] reported an experimental study on pressure loading of detonation waves through 90-degree bend and got a conclusion that a high pressure peak arises at the extrados of the bend and a double pressure peak occurs just downstream of the bend outlet due to transverse wave propagation.

Detonation propagation through a bend which is of vital importance to industrial safety is more complicated than that in a straight pipe due to detonation reflection and diffraction involved. Although many literatures refer to detonation propagating through a bend numerically or experimentally, study of the evolving detonation cell structure involved physical mechanism still need to be investigated in detail and systematically. In the present work, the cellular detonation propagating through a smooth pipe bend with different angles is investigated for the wave dynamic processes including both reflection and diffraction. The numerical scheme employed is the fifth order Weighted Essentially Non-Oscillatory (WENO) scheme and IMEX Additive Runge-Kutta (ARK) methods considering the stiffness of the reactive source terms. A detailed elementary chemical reaction model is also implemented.

2 Numerical modeling

2.1 Governing equations

The model for detonation propagation in a stoichiometric H₂-O₂ mixture diluted by 70% Ar is the reactive Euler equations for multi-species with source terms. In 2-D general coordinates, these equations in which the effect of viscosity, the heat transfer, the diffusion and body forces are neglected can be written as a conservation law of the form,

$$\frac{\partial \tilde{U}}{\partial \tau} + \frac{\partial \tilde{F}}{\partial \zeta} + \frac{\partial \tilde{G}}{\partial \eta} = \tilde{S} \quad (1)$$

$$\tilde{U} = \frac{U}{J}, \quad \tilde{F} = \frac{1}{J}(\xi_x F + \xi_y G), \quad \tilde{G} = \frac{1}{J}(\eta_x F + \eta_y G), \quad \tilde{S} = \frac{S}{J}, \quad J = \left| \frac{\partial(\xi, \eta)}{\partial(x, y)} \right|, \quad (2)$$

where, J is the Jacobian determinant. (ζ, η) and (x, y) are coordinates of Descartes and general coordinates, respectively. $\xi_x, \xi_y, \eta_x, \eta_y$ are metrics of transformation of coordinates. A detailed chemical reaction model comprised of 9 species and 48 elementary reactions [5] was employed here for describing H₂-O₂-Ar detonation.

2.2 Numerical methods

Considering the stiffness of the reactive source terms, the Additive Runge-Kutta (ARK) method [6] is adopted in this work to couple the Euler equations to the chemical reactions. The reactive equation in ARK methods can be written as $U_t = L(U) + S(U)$, in which $L(U)$ and $S(U)$ represent the non-stiff and stiff terms, respectively. Each time step in ARK is calculated by,

$$\begin{cases} U^{(i)} = U^n + \Delta t \sum_{j=1}^{i-1} a_{ij} L(U^{(j)}) + \Delta t \sum_{j=1}^i \hat{a}_{ij} S(U^{(j)}), & i=2,3,\dots,s, \\ U^{n+1} = U^n + \Delta t \sum_{j=1}^s b_j L(U^{(j)}) + \Delta t \sum_{j=1}^s \hat{b}_j S(U^{(j)}) \end{cases} \quad (3)$$

where, each of the two terms is integrated by its own s -stage Runge-Kutta method. None that, $U^{(i)} = U(t^n + c_i \Delta t)$ is the value of the U on i -th stage, and $U^{n+1} = U(t^n + \Delta t)$. For each i -th stage, if source term S is an implicit function of U , $U^{(i)}$ is implicitly computed by Newton iteration.

2.3 Initial and boundary conditions

The numerical simulation was conducted to reveal the evolution of cellular detonation wave propagating through realistic smooth pipe bends with different bend angles in 2-D. The pipe was filled with a stoichiometric H₂/O₂ mixture diluted with 70% Ar at an initial pressure and temperature of 6.67KPa and 298K, respectively. The entire pipe consisted of a straight tube section, a bend section, and a sloped tube section. The bend angle θ was varied from 30° to 90°. The grid size was fixed at 0.2mm. To be able to obtain a 2D regular cellular detonation wave, a 1-D ZND detonation wave was mapped onto a 2-D straight duct domain. This initial detonation wave would evolve into a stable triple-shock structure after introducing some unreacted gas pockets behind the detonation front. The resulting stable 2D detonation wave with regular cellular structure subsequently propagated from the straight-duct section of the tube of width 5λ ($\lambda=7.2\text{mm}$) through a pipe bend of arc length 6.66λ . Three bend angles, i.e., 30°, 60° and 90°, were studied in this work. The extrapolation boundary condition and the Neumann boundary condition were applied at inlet and outlet, respectively. The solid wall boundary conditions were used at the upper and lower walls.

3 Code verifications

The effects of grid size on detonation parameters were illustrated in one-dimensional gaseous detonation. The results are summarized in Table 1. Fig.1 shows some characteristic parameters of the cellular pattern, including exit angle α , the ratio of cell width to cell length λ/l , entrance angle β and angle of transverse wave trace ω . Parameters comparison listed in Table 2 show that the computed cells solution agrees well with experiment ones in quantity.

Table 1 Calculated detonation parameters with different grid sizes

Grid size (mm)	Detonation velocity (m/s)	C-J pressure (Pa)	Wall pressure (Pa)	V-N pressure (Pa)	Reaction zone length (mm)	Induction zone length (mm)
2	1,620	93,600	35,830	135,000	28	—
1	1,620	93,600	35,830	149,000	18	—
0.5	1,620	93,600	35,830	159,000	15	—
0.2	1,620	93,600	35,830	166,000	12	1.9
0.1	1,620	93,600	35,830	169,000	10	1.6
0.05	1,620	93,600	35,830	172,000	10	1.5

Table 2 Parameters comparison of the computed cells solution with experiment ones.

Cell structure parameters	Computation results	Experiment [8-9]
λ/l	0.6	0.5-0.6
α	10	5-10
β	35-42	32-40
ω	~ 32	~ 30

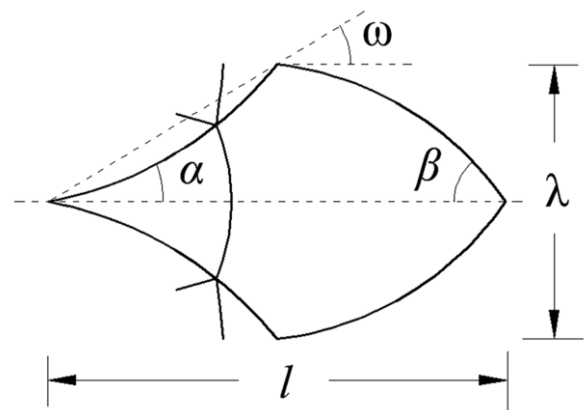


Figure 1 Some characteristic parameters of the cell.

4 Results and discussions

Fig.2 shows the detonation cells pattern when the regular detonation wave propagates through the pipe bend with bending angle $\theta = 30^\circ$. The whole domain can be divided into four regions, demarcated by A, B, C and D. The detonation cells in region A is regular and approximately 7.2mm wide and 12.96mm long. However in region B, the detonation cells lose their regularity as a result of the diffraction and reflection effects. In the upper half of region B, the diffraction near the inner wall causes the decrease of pressure which leads to an increase in cell size. On the contrary, the cell size in the lower half of region B is growing smaller owing to the mach reflection occurred on the outer wall of the bend. In region C, after complicated triple points collision and interaction, these detonation cells re-obtain their regularity and have the same size with those in region A. So there is a transition length defined as the distance from outlet of the bend to region D. In the case with bending angle $\theta = 30^\circ$, the length of transition length is approximately 0.32m. With $\theta = 30^\circ$, when the regular detonation wave moves into and compacts with the bend, it get compressed near the outer wall at the bottom, thus the maximum pressure arises from 2.5atm to 3.5atm, which can be found from the red line in Fig.6(a). Near the inner wall, continuous shock diffraction leads to the maximum pressure slightly drops to 2.3atm which is greater than the pressure limit of detonation. That is why the detonation is not failed near the inner wall and moves forward to the next section.

Similar to Fig.2, the whole domain in Fig.3-4 also can be divided into four regions. However, with the bend angle increasing from $\theta = 30^\circ$ to $\theta = 90^\circ$, the Mach reflection occurred on the outer wall grows stronger and creates a highly overdriven detonation wave, especially in Fig.4 with bending angle $\theta = 90^\circ$. The detonation cells have smaller size and the then disappear with the detonation wave moving past the whole bend, with the same time, the detonation wave completely fails near the inner wall due to stronger expansion wave caused by diffraction and decouple zone exists. It is clearly seen from Fig.6(c) that the green line that the maximum pressure decreases to an extremely low value, then the detonation could not keep self-sustained and fails. The reason for the detonation failure near the

inner wall on the bend is that the continuous rarefaction wave generated by diffraction causes the pressure decrease below the detonation limit that leads to decoupling of shock and reaction front.

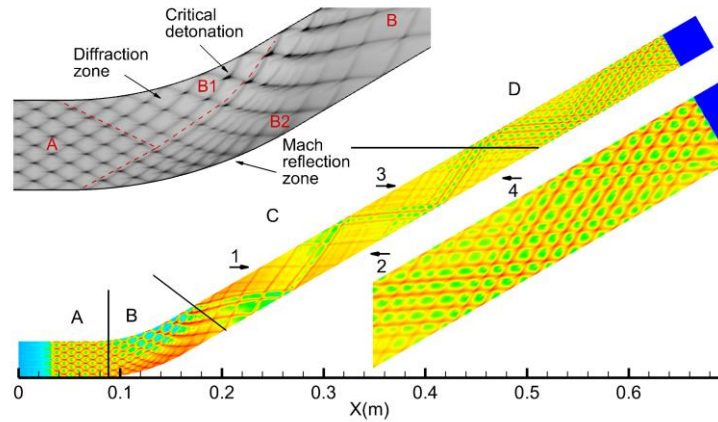


Figure 2. Detonation cells pattern for regular detonation propagating through a 30° angle pipe bend of 5λ width. The upper graph is an enlargement of the cell pattern in the bend. The lower graph is an enlargement of the cell pattern in Region D.

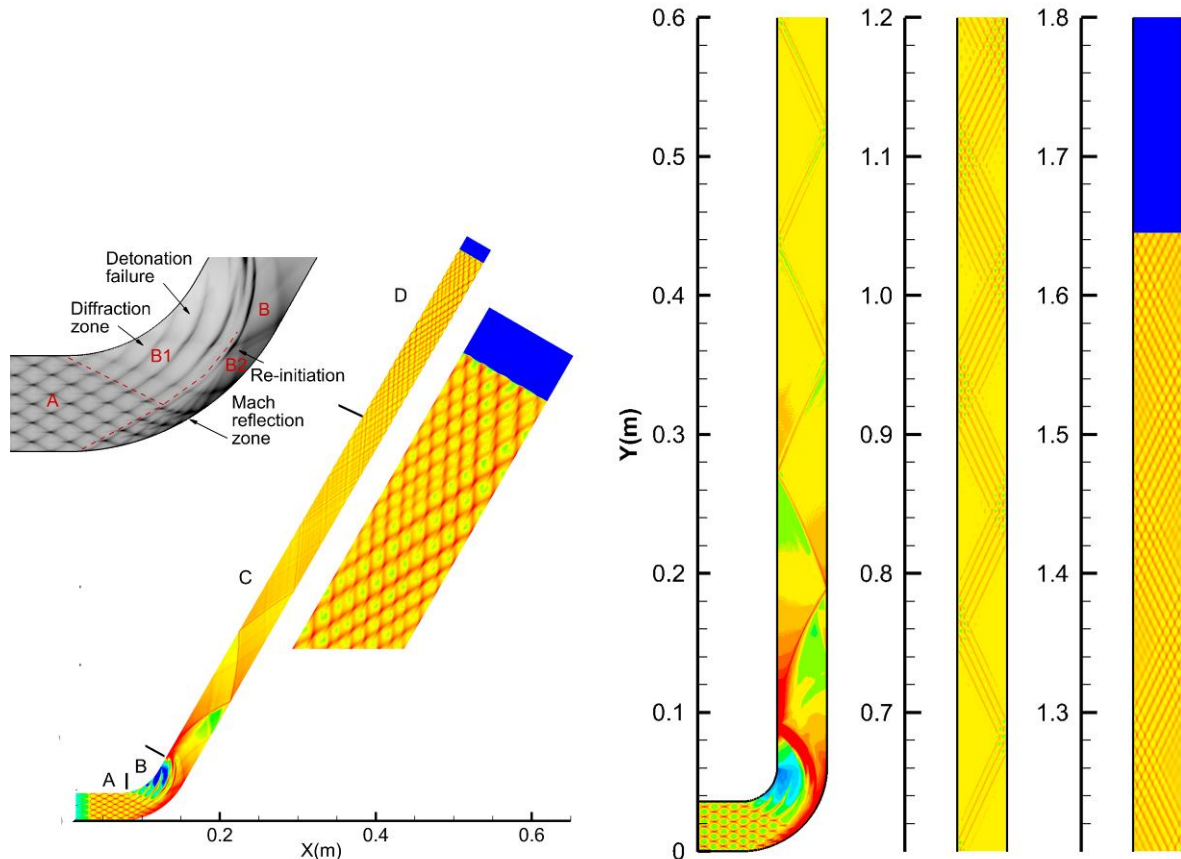


Figure 3 Detonation cells pattern for regular detonation propagating through a 60° angle pipe bend of 5λ width. The upper graph is an enlargement of the cell pattern in the bend. The lower graph is an enlargement of the cell pattern in Region D.

Figure 4 Detonation cells pattern for regular detonation propagating through a 90° angle pipe bend of 5λ width.

The upper graph in Fig.2-3 and Fig.5 shows three profiles of detonation cell pattern in the bend with bending angle $\theta = 30^\circ$, 60° and 90° . There is a clearly visible difference in detonation cell pattern

denote by the red dash line between region A and B. in region B, upper half is diffraction zone (B1) and lower half is mach reflection half (B2). It's well known from the previous researches that mach reflection of detonation occurs depending on whether the wedge angle is less than critical angle θ_c . According to [7], $\theta_c = 46^\circ$. A conclusion can be got that mach reflection occurs on outer wall at the very beginning until the turning point located at the cross section 46° from bend inlet. We can found that the detonation cells pattern near the outer wall is regular when the radius angle of concave surface is less than 46° , then becomes more irregular and disappears with the radius angle of concave surface is greater than 46° . The triple point trajectories under the reflected main triple point trajectory are convergent. This is evidently different from detonation reflection from a wedge, in which the triple point trajectories are parallel with each other behind the reflected mach stem.

Table 3 lists the length of transition region, the ultimate cell size and the width/length ratio at various bending angle. It is easily discerned that as the bending angle increases, the length of transition region gets longer, but the ultimate cell size is considerably affected by the bending angle, the width/length ratio tends to be approximately constant and the shape of the detonation cells remains the same.

Table 3: Transition region and ultimate cell size various sloping angles

Sloping angle	Length of transition region (m)	Ultimate cell size (mm)		Width/length ratio
		Width	Length	
30°	0.32	7.2	13.05	1.812
60°	0.52	6.1	11.01	1.805
90°	1.12	5.9	10.68	1.810

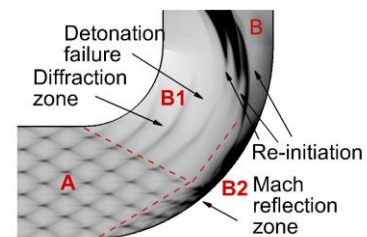


Figure 5 An enlargement of the cell pattern in the bend of Fig.4.

Not only focusing on the cellular structure, the detonation wave structure involving physical process is also investigated in detail as it undergoes the diffraction and reflection. After the detonation wave exiting the bend outlet, all transverse waves near the outer wall propagated upward, as shown in Fig.7 (a). The transverse wave of the first triple point got compressed by adjacent approaching waves and became more wrinkled as the wave propagated further. In addition, a secondary triple point was created on the transverse detonation by the transverse wave itself and propagated toward the first triple point (Fig.7(c)-(d)), another wrinkle occurred subsequently behind the secondary triple point on the same transverse wave. Finally, the secondary triple point merged with the first triple point and created a more flat transverse detonation wave (Fig.7 (e)). Right before the transverse detonation wave impacted on the upper wall, a tertiary triple point emerged. In summary, a transverse wave could become wrinkled and eventually new triple points could be created due to continuous compression by other transverse waves propagating right behind.

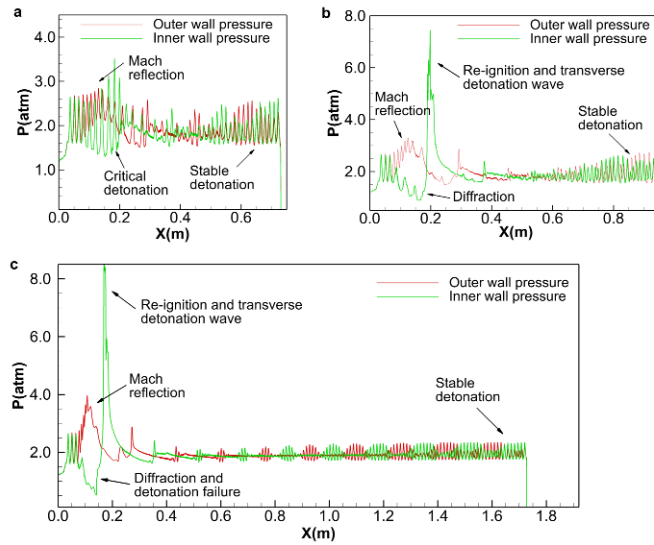


Figure 6 Maximum pressure histories on inner and outer wall. (a- $\theta = 30^\circ$, b- $\theta = 60^\circ$, c- $\theta = 90^\circ$)

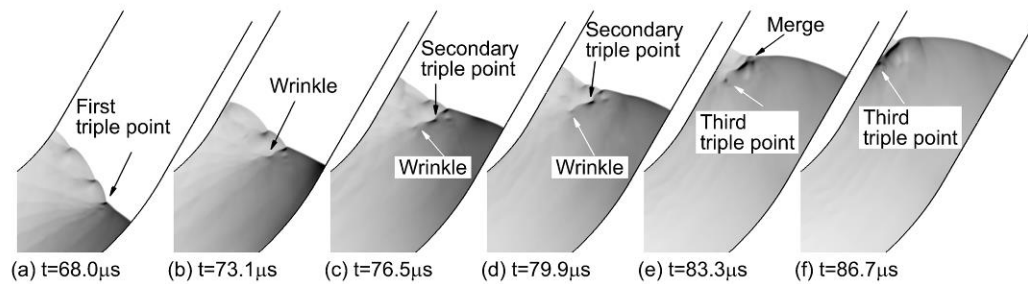


Figure 7 Schlieren plots of the pressure ($\theta = 60^\circ$).

4 Conclusions

Numerical simulation of cellular detonation wave propagating through a smooth pipe bend with bending angle $\theta = 30^\circ, 60^\circ, 90^\circ$ have been performed by ARK methods with a detailed chemical reaction model. The following conclusions are derived that detonation compaction with smooth bend is a combination of diffraction and reflection which increases the cell size near the inner wall and decreases the cell size near the outer wall respectively. With bend angle increasing, continuous expansion wave can make the detonation from critical detonation to failure near the inner wall and partial detonation fails near the outer wall. There exists a transition length before the detonation re-obtains its regularity after the detonation moving out of the bend as the detonation exits the bend outlet.

Acknowledgments

This work was supported by the National Basic Research Program of China (No. 2010CB832706), National Natural Science Foundation of China (No. 11032002).

References

- [1] Nettleton MA. (2002). Recent work on gaseous detonation. Shock Waves. 12:3.

- [2] Thomas GO, Williams RL. (2002). Detonation interaction with wedges and bends. *Shock Waves*. 11:481.
- [3] Deiterding R. (2009). A parallel adaptive method for simulating shock-induced combustion with detailed chemical kinetics in complex domains. *Comput. Struct.* 87:769.
- [4] Uchida M, Suda T, Fujimori T, et al. (2011). Pressure loading of detonation waves through 90-degree bend in high pressure H₂-O₂-N₂ mixtures. *Proc. Combust. Inst.* 33:2327.
- [5] Westbrook CK. (1982). *Chemical Kinetics of Hydrocarbon Oxidation in Gaseous Detonations*. Combust. Flame. 46:191.
- [6] Kennedy CA, Carpenter MH. (2003). Additive Runge-Kutta schemes for convection-diffusion-reaction equations. *Appl. Numer. Math.* 44:139.
- [7] Qu Q, Khoo BC, Dou HS, Tsai HM. (2008). The evolution of a detonation wave in a variable cross-sectional chamber. *Shock Waves*. 18:213.
- [8] Wang G, Wang J T, Liu K X. (2009). New numerical algorithms in SUPER CE/SE and their applications in explosion mechanics. *Sci China Ser G*, 39: 1214.
- [9] Hu X Y. On the structures of gaseous detonation waves. (2001). The Institute of Mechanics, Chinese Academy of Sciences, Beijing.